Macromolecules

ARTICLE

pubs.acs.org/Macromolecules

Specific Salt Effects on Poly(ethylene oxide) Electrolyte Solutions

Chun-lai Ren,[†] Wen-de Tian,[‡] Igal Szleifer,[§] and Yu-qiang Ma*[,†,‡]

[†]National Laboratory of Solid State Microstructures, Nanjing University, Nanjing 210093, China

[‡]Center for Soft Condensed Matter Physics and Interdisciplinary Research, Soochow University, Suzhou 215006, China

[§]Department of Biomedical Engineering, Northwestern University, 2145 Sheridan Road, Evanston, Illinois 60208, United States

ABSTRACT: Exploring the mechanism of specific salt effects in electrolyte solutions is an old and attractive subject. It has been gradually realized that the competition at the molecular level plays an important role. Aiming to include molecular details as many as possible, we combine molecular dynamics (MD) simulations with a molecular theory to study specific salt effects on poly(ethylene oxide) (PEO) solutions with the addition of monovalent salt. Radial distribution functions obtained from MD simulations provide microscopic structures of different components as well as interactions between various species. On the basis of these interactions, we construct the molecular theory with four assumptions: (1) an ion along with bound water in the first shell works as a single entity; (2) short-ranged interactions among various species are modeled as hydrogen-bonding interactions; (3) the ability of a hydrated ion to provide donors/acceptors for hydrogen bonding is governed by the charge density; (4) contact ion pairs are included, especially in the cases of small cations. The molecular theory is generalized with the explicit inclusion of ion−PEO, ion−water, ion−ion, water−water, and water−PEO hydrogen bonds. This means the molecular-scale structure and interaction are included within the frame of the theory. Theoretically calculated cloud points verify that the salting-out ability for alkali metal ions follows the series of $K^+ > Rb^+ > Cs^+ > Na^+ > Li^+$, which is in agreement with the experimental observations. Here, the competition among ion−PEO, ion−water, and water−PEO interactions and the impact of steric repulsions induced by the introduction of ions are two essential factors determining the phase behavior of PEO solutions. The combined methods bridge the microscopic interactions and structures to the macroscopic behavior.

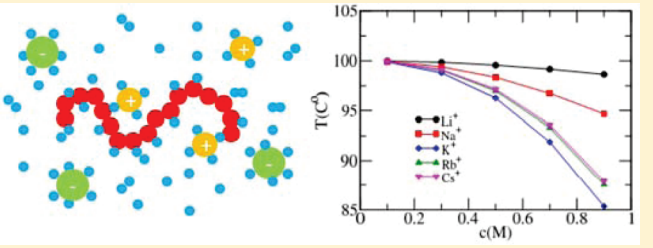

I. INTRODUCTION

Poly(ethylene oxide) (PEO) has good solubility in water at room temperature and undergoes phase separations at high temperatures. And at even higher temperatures, PEO shows good solubility again.[1−4] The aqueous two-phase systems have been successfully used for the separation of biological materials as a nondenaturing environment.[5,6] Both for the academic interest in the loop behavior of phase diagrams and for the practical importance in chemistry, biology, and food science, numerous fundamental studies, including experiments,[7−9] theories,[10−14] and computer simulations,[15−18] have been published during recent decades. The mechanism of the phase separation in PEO solutions is attributed to the competition between the formation of water−PEO and water−water hydrogen bonds. Moreover, PEO is the one of stimuli-responsive polymers whose behaviors largely depend on environment conditions, such as temperature, pH, and salt concentration.[19] Experiments have shown that either the cloud point or the viscosity of PEO solutions changes dramatically with the addition of salts.[20−25] The explanation given by previous work[20] suggested the existence of a salt-deficient zone near the polymer. Although these ideas were used to predict the decrease of cloud point as the salt concentration is increased, the mechanism at the molecular level is still unclear. In order to disclose it, two basic questions need to be answered properly: (1) what is the salt effect on water, and (2) what is the salt effect on PEO?

The first question was addressed more than 100 years ago.[26] Traditionally, ions are divided into two groups according to the ways that they change water structure.[27−31] One group is structure-making, which strengthens water−water hydrogen bonds and leads to more ordered water structure. The other is structure-breaking, which weakens water−water hydrogen bonds and results in more disordered water structure. The Hofmeister series has been concluded to rank the ability of ions to change water structure based on experimental observations. Interestingly, the series is quite universal in various systems, such as protein precipitation,[32] enzyme activity,[33] bacterial growth,[34] and so on. However, these empirical conclusions are insufficient to provide the subsequent physical pictures originating in the subtle interactions at the molecular level. The microscopic mechanism of the Hofmeister series has started to be uncovered during the past 25 years with the development of new techniques and computers. Unfortunately, the new perspective provides a different picture from the traditional explanation.[35−39]

Received: December 6, 2010
Revised: January 14, 2011
Published: February 14, 2011

A fundamental point of view is that the effect of ions on water structure is very local, not global, as supported by recent experiments[40−43] and simulations.[44−47] It turns out that the concept of structure-making and structure-breaking is misleading, since the change of water structure caused by the presence of ions was exaggerated.

The second question relates to the specific nature of the solute and to the fact that specific salt effects usually depend on distinct salt−solute interactions. For instance, researchers[48,49] investigated hydrophobic interactions between hydrophobic particles and found different salt effects depending on the size of particles. Another experiment[50] studied the salt effects on the lower critical solution temperature (LCST) of PNIPAM and showed the decrease of LCST caused by anions in different ways relying on various anion−PNIPAM interactions. Furthermore, it was observed[51] that the deswelling extent of poly(styrenesulfonic acid) (PSSA) hydrogel in solutions with selected cation chloride salts deviates, and in some cases even reverses, the expectations from the Hofmeister series. These findings were attributed to specific interactions between ions and PSSA. Hence, it has been accepted that the Hofmeister series may have different origins based on various salt−solute interactions,[39,52] which implies that specific ion−solute interactions should be considered properly in order to get the correct mechanism of specific salt effects in different systems. However, it is a complicated task to describe the subtle interactions in electrolyte solutions due to the existence of multiple components.

Various theoretical models have been put forward in the field. In order to fit experimental data, semiempirical models[20,53−56] have been established, which include some adjustable parameters because of the lack of microscopic knowledge. Instead, a statistical mechanical modeling[57,58] is a more consistent way. However, one big challenge is how to describe the molecular-scale structures and interactions. To overcome it, we first perform MD simulations on PEO electrolyte solutions. At this stage, microscopic structures and interactions of each type of molecule can be obtained by the analysis of radial distribution functions (RDFs). Second, we are able to establish a statistical thermodynamic theory based on the knowledge of molecular-scale structures and interactions. Moreover, the size, shape, and conformation of each molecular type are considered explicitly within the frame of molecular theory. Third, cloud points of PEO electrolyte solutions can be calculated from the theory as well as microscopic information. By comparing the theoretical results with experimental measurements and analyzing microscopic interactions, we can explore the molecular mechanism of the specific salt effects on PEO electrolyte solutions.

II. MD SIMULATIONS

MD simulations are performed on PEO electrolyte solutions at a fixed PEO concentration of 1 wt % and temperature of 100 °C. Two polymer chains with the number of segment $N = 25$ and more than 6000 water molecules are included. Five types of salts are studied, which are LiCl, NaCl, KCl, RbCl, and CsCl. Salt concentrations are chosen within the range of 0−1 M. OPLS-AA[59−62] force fields are used for PEO chains and salts, and the model for water is TIP4P. First, we perform NPT simulations over 4 ns to reach equilibrium densities at a pressure of 1 bar. The production runs are preformed in the NVT ensemble over 30 ns. All simulations are carried using the GROMACS 4.0.7 package.[63]

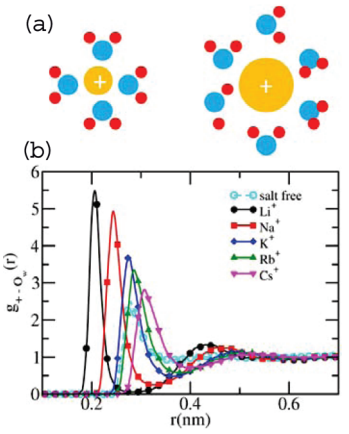

Figure 1. (a) Schematic representation of bound water within the first hydration shell around cations of different sizes. Orange, blue, and red spheres represent cation, oxygen, and hydrogen of water, respectively. (b) Cation−oxygen radial distribution functions at the salt concentration of 0.5 M. Solid lines with symbols are for five different cations: circle for Li^+, square for Na^+, diamond for K^+, triangle up for Rb^+, and triangle down for Cs^+. The dashed line with open circle is the oxygen−oxygen radial distribution function in the salt-free case.

Figure 1a provides a schematic representation of the formation of the first solvation shell around the ions, where bound water molecules are oriented around the small cation, and thus the electric field of the ion is efficiently shielded by the reorientation of bound water.[62,64−67] The hydrated structures of alkali mental ions are well reflected by cation−oxygen radial distribution functions in Figure 1b. The common character of these five RDFs is that the first peak is very pronounced, while the second is weak. It confirms the view reported in the previous paper[38] that monovalent ions only affect the first water layer. From Li^+ to Cs^+, the first peak becomes lower and further away, indicating the decaying ion−water interaction and the loosing of the hydration shell as the size of cation is increased.

It is known that within the first hydration shell both ion−water and water−water interactions are important. To compare these two types of interactions, the oxygen−oxygen RDF for the case of salt free is given in Figure 1b. We find that the peak of oxygen−oxygen RDF occurs between the one of K^+−oxygen and that of Rb^+−oxygen RDFs, which indicates that ion−water interaction is stronger than water−water interaction in cases of Li^+, Na^+ and K^+, while the opposite is true for Rb^+ and Cs^+. This fact also explains why water molecules are weakly bound around large cations. Similar results were obtained in previous studies,[68−70] which suggested that water molecules are strongly bound only within the first hydration shell of small cations.

According to the existence of the important first peak of cation−oxygen RDFs in Figure 1b, we can argue that the water molecules in the vicinity of ions are closed packed. That is to say, the local water structure around ions changes dramatically, as compared to the pure water. The question that arises then is: do ions have the ability to change the global water structure? Figure 2 shows (a) oxygen−hydrogen RDFs and (b) oxygen−oxygen RDFs with and without salt, where they display very similar behavior. Here we check the water structure with different salt concentrations in the range of 0−1 M and find they are almost identical to the salt-free condition. This finding supports the

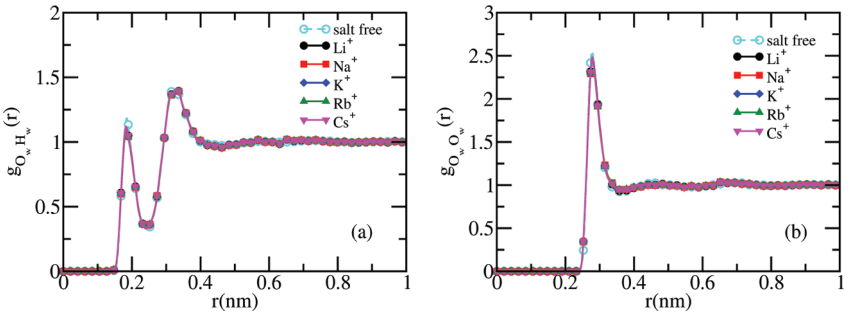

Figure 2. (a) Oxygen−hydration and (b) oxygen−oxygen radial distribution functions at the salt concentration of 0.5 M. The dashed line with open circle is the salt-free case.

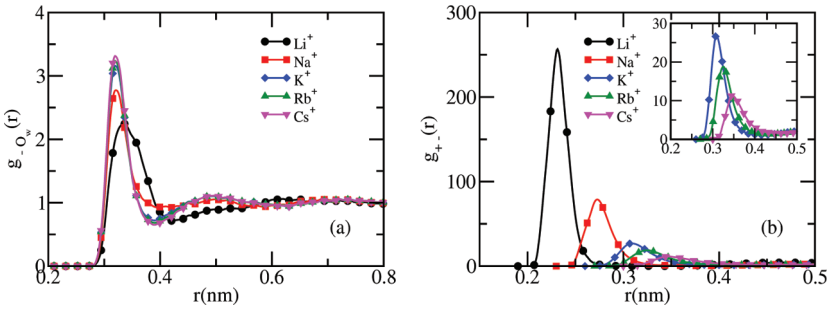

Figure 3. (a) Anion−oxygen and (b) cation−anion radial distribution functions with the inset of enlarged RDFs for large cations at the salt concentration 0.5 M.

point of view that ion effects on the water structure are very local.[35−39] Our conclusion is also in agreement with the data by Bouazizi et al.,[71,72] where the salt effects on water structure were systematically investigated for LiCl solutions[71] and NaCl solutions[72] by combining X-ray scattering and molecular dynamics simulations. They provided similar behaviors of $g_{O_wH_w}(r)$ and $g_{O_wO_w}(r)$ without and with salt under medium salt concentrations, as obtained in Figure 2. Particularly, we get positions of the first peak of $g_{O_wH_w}(r)$ (and $g_{O_wO_w}(r)$) at 0.183 nm (and 0.278 nm), which agree with the results obtained from LiCl solutions[71] (0.180 and 0.277 nm) and NaCl solutions[72] (0.177 and 0.277 nm) well. Thus, only the local order of water structure is induced by the addition of monovalent ions in the solutions. Given this fact, it is reasonable for us to consider an ion with bound water in its first solvation shell as a single entity. Usually, the size of the hydrated ion is defined as the first minimum of ion−oxygen RDF.

Anion−oxygen RDFs in Figure 3a provide the hydrated structure of chloride in the five cases of different cations. It may be expected that the distribution would be similar. However, we find that only for large cations (i.e., K^+, Rb^+, and Cs^+) chloride−oxygen RDFs are the same. The case of Li^+ displays a very different behavior as compared to the others, where the height of the peak is lower and the width is larger. The distribution for the case of Na^+ shows a small deviation as compared to the larger cations. These findings imply that there is a coupling between cation and anion structures and hydration for small cations. In order to better understand the coupling between cation and anion, their mutual RDFs are shown in Figure 3b. The figure shows that the peak of $g_{LiCl}(r)$ is very large, followed by that of $g_{NaCl}(r)$, as compared to those in large cation cases in the inset. As the closest distance between cation and anion for Li^+ and Na^+, seen in Figure 3b, is compatible with the distance between cation and the oxygen of water, seen in Figure 1b, we suggest the existence of contact ion pairs, as reported in previous papers.[65,73,74] The ion pairs result from the strong attractions between cations and anions, and they are more prevalent for small cations, where the interaction at contact becomes very large due to the $1/r$ dependence of the electrostatic potential. The ratio of contact ion pairs to the total number of ion can be calculated by integrating cation−anion RDFs to the first maximum,[65] which is shown in Table 1.

Table 1. Ratio of Contact Ion Pairs in Li^+ and Na^+ at Different Salt Concentrations

	c (M)				
	0.1	0.3	0.5	0.7	0.9
Li^+	0.41	0.50	0.52	0.54	0.56
Na^+	0.10	0.18	0.24	0.27	0.31

So far we have investigated the structure and interactions of ions and water. Next we discuss the behavior of the polymers, poly(ethylene oxide), in the salt solutions. Parts a and b of Figure 4 provide the RDFs of EO−hydrogen and EO−EO, respectively. The positions of the first peak of EO−hydrogen RDFs appear at $r = 0.2$ nm, while those of EO−EO RDFs happen at $r \sim 0.5$ nm. This implies the fact that hydrogen bonds are formed between the oxygen of EO segments and the hydrogen of water molecules. The height of a tiny peak in the vicinity of the EO segment in Figure 4a reflects the extent of water−PEO hydrogen binding. To verify the validity of the present simulation, we try to compare our results on the salt-free case with the work by Smith et al.,[18] where the hydrogen binding behavior of

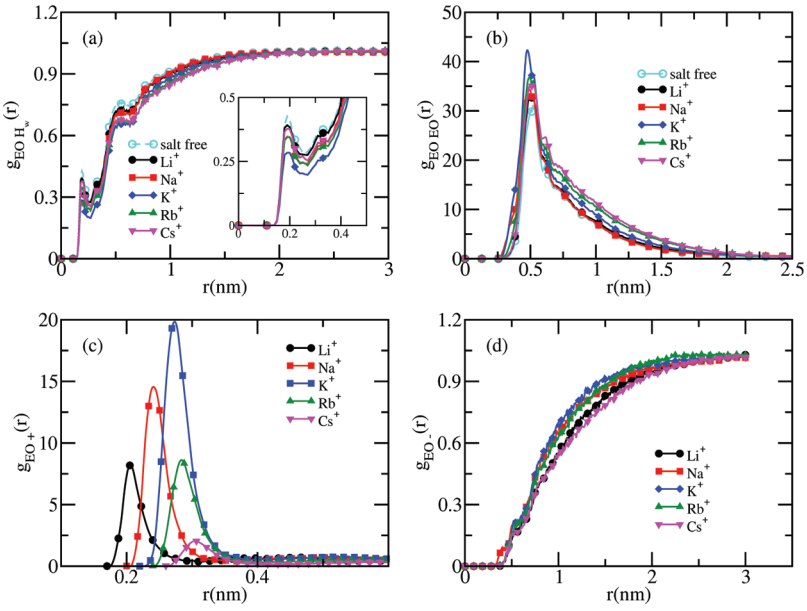

Figure 4. Radial distribution functions of (a) EO−hydrogen with the inset of enlarged first peaks, (b) EO−EO, (c) EO−cation, and (d) EO−anion. The salt concentration is 0.5 M.

PEO solutions was successfully studied. Following the definitions of water−PEO (and water−water) hydrogen bonds (hbs) by Smith et al., we show that positions of the first minimum of $g_{EOH_w}(r)$ (and $g_{O_wH_w}(r)$) are at 0.26 nm (and 0.24 nm) and numbers of water−PEO (and water−water) hbs are 1.14 (and 1.65) for the PEO solution with the concentration of 1 wt % and at the temperature of 100 °C. These results are very close to those obtained by Smith et al., indicating that the formation of water−water hydrogen bonds is stronger than that of water−PEO hbs; namely, the first peak of EO−hydrogen RDF is tiny. After the addition of salt, we find that water−PEO hydrogen bonds tend to be broken. Moreover, the ability to break water−PEO hbs for various cations is different. In the inset of Figure 4a we observe that from Li^+ to Na^+ to K^+ the extent of breaking water−PEO hbs is strengthened. But from K^+ to Rb^+, and to Cs^+, the extent is weakened. Thus, water−PEO hbs decrease mostly in K^+. To further study the influence of salt on PEO, EO−cation RDFs and EO−anion RDFs are provided in parts c and d of Figure 4, respectively. The appearance of the peak in Figure 4c indicates the existence of cation−PEO association, as has been observed in experiments.[75] As the position of the peak is smaller than 0.4 nm, the interaction between cation and PEO is short-ranged. Given the fact that ions are bound with water molecules, the simulations indicate that hydrogen bonds are formed between the oxygen of an EO segment and the hydrogen of water. Furthermore, the number of cation−PEO bonds is found to strongly depend on the type of cations. Figure 4c shows that EO−K^+ binding is the strongest. Combining parts a and c of Figure 4, we conclude that the more EO−cation bonds form, the more water−PEO hydrogen bonds break. Figure 4d presents EO−anion RDFs, where no peak appears. This means, as expected, that there are no attractions between PEO and anion.

To summarize, MD simulations provide molecular details about the microscopic structures and interactions of different molecules, which are very useful for the development and application of the following theoretical modeling.

Table 2. Radius, Coordinate Number, and Number of Donors and Acceptors per Bound Water, Where the Unit of Radius Is nm[a]

	Li^+	Na^+	K^+	Rb^+	Cs^+	Cl^-
size	0.28	0.33	0.37	0.39	0.40	0.39
CN	3.0	5.0	6.0	7.0	7.5	7.0
donor	2	2	2	1	1	0
acceptor	0	0	1	1	1	2

[a] For explanation see Appendix.

III. MOLECULAR THEORY

We are interested in treating PEO electrolyte solutions, which are composed of PEO, water, cation, and anion. Inspired by the results from the MD simulations ions in the theoretical development should be treated as hydrated ions, i.e., an ion with bound water molecules within the first hydration shell. Furthermore, the coupling between cation and anion in small cations (Li^+ and Na^+) requires that we take the contact ion pair into account as an additional species. The numbers of different species—PEO, water, hydrated cations, hydrated anions, and ion pairs—are given by N_{pol}, N_w, N_+, N_-, and N_{+-}, respectively. The chain of PEO has N segments, each with a volume v_p. The volume of water is v_w. The geometry of cation/anion is assumed to be spherical, with the radius determined by the first minimum of cation−oxygen/anion−oxygen RDFs. Contact ion pairs are modeled(simplified) as spheres, too, with the radius at the first maximum of cation−anion RDFs.

The Helmholtz free energy density, free energy divided by the total volume V, of the system has the following contributions:

$$\frac{\beta F}{V} = -\frac{S_{con}}{k_B V} - \frac{\sum_i S_i}{k_B V} + \frac{\beta F_{inter}}{V} + \frac{\beta F_{assoc}}{V} + \frac{\beta U_{rep}}{V} + \frac{\beta F_{elec}}{V} \quad (1)$$

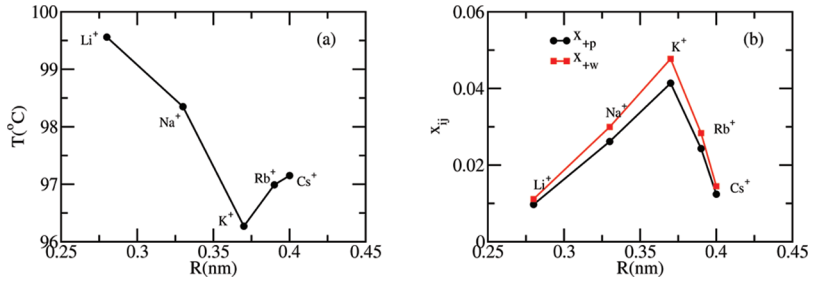

Figure 5. (a) Cloud points of PEO solutions with PEO:water = 1 wt % with the salt concentration of 0.5 M. (b) Average fractions of cation−PEO (x_{+p}) and cation−water (x_{+w}) hydrogen bonds with the salt concentration of 0.5 M and the temperature of 100 °C.

The first term in eq 1 denotes the conformational entropy of polymer chains, which is given by

$$\frac{-S_{con}}{k_B V} = \frac{\rho_p}{N}\sum_{\alpha} P(\alpha)\ln P(\alpha) \tag{2}$$

where $P(\alpha)$ is the probability distribution function (pdf) of finding a chain in conformation α, and the density of EO segments is ρ_p.

The second term of the free energy describes the translational entropy of the five species in the system.

$$-\frac{\sum_i S_i}{k_B V} = \frac{\rho_p}{N}\left[\ln\frac{\rho_p}{N}v_w - 1\right] + \rho_w[\ln \rho_w v_w - 1] + \rho_+[\ln \rho_+ v_w - 1] + \rho_-[\ln \rho_- v_w - 1] + \rho_{+-}[\ln \rho_{+-} v_w - 1] \tag{3}$$

where ρ_i (i = p, w, +,−,+ −) are densities of different species, respectively. Volume fractions can be expressed as $\phi_i = \rho_i v_i$, where v_i represents the volume of each molecule.

The third term describes the effective intermolecular interaction of PEO in the solution, which accounts for the solvent quality, and it is expressed by

$$\frac{\beta F_{inter}}{V} = \frac{\chi}{v_w}\phi_p(1-\phi_p) \tag{4}$$

where χ is a generalized Flory−Huggins-type parameter with the expression of $\chi = B/T$. The temperature is T, and B is a constant.

The fourth term accounts for short-ranged hydrogen-bonding interactions. In a pure PEO solution, only water−PEO and water−water hydrogen bonds need to be considered. After salts are added, additional hydrogen bonds including water−ion, ion−PEO, and ion−ion should be taken into account. According to previous works,[14,76] the free energy arising from the formation of different kinds of hydrogen bonds is

$$\beta F_{assoc} = -\ln Z_{assoc} \tag{5}$$

where Z_{assoc} is a partition function and equals to

$$Z_{assoc} = P_{comb}\prod_{i,j} W_{ij}\exp(\beta\Delta E_{ij} n_{ij}) \tag{6}$$

Here P_{comb} is a combinatorial factor, which describes the number of ways to form n_{ij} hydrogen bonds between species i and j, where i is a donor and j is an acceptor. For a specific type of molecule, it is assumed to provide d_i donors and a_j acceptors. Consequently, the combinatorial factor becomes[77]

$$P_{comb} = \prod_{i=1}^{k}\frac{(N_i d_i)!}{(N_i d_i - \sum_{m=1}^{k} n_{im})!}\prod_{j=1}^{k}\frac{(N_j a_j)!}{(N_j a_j - \sum_{l=1}^{k} n_{lj})!}\prod_{i=1}^{k}\prod_{j=1}^{k}\frac{1}{(n_{ij})!} \tag{7}$$

W_{ij} in eq 6 is a probability of finding a donor i and an acceptor j in the vicinity of each other and in the correct orientation to form a hydrogen bond. The probability is expressed as[14]

$$W_{ij} = \left(\frac{v_{hb}^{ij}}{V}\right)^{n_{ij}} \tag{8}$$

where v_{hb}^{ij} is a volume of the hydrogen bond between i and j. In eq 6 ΔE_{ij} is an energetic gain associated with the formation of the hydrogen bond.

To determine the free energy of hydrogen bonding, the number of donors/acceptors offered by each type of species should be known. An EO segment has two donors. A free water molecule acts as two donors and two acceptors. For various ions, Table 2 gives the radius, coordinate number, and the number of donors/acceptors provided by each bound water molecule. The radius of ions is defined as the first minimum of ion−oxygen RDFs. The coordinate number (CN) is obtained by the integration of RDFs to the first minimum, which depends on the salt concentration and temperature. According to our simulations, when the salt concentration varies in the range of <1 M at the temperature of 100 °C, the change of CN is less than 0.5. Table 2 gives the average number of CN for different conditions. We get the number of donors/acceptors of different ions by multiplying the coordinate number with the number of donors/accepteors per bound water, except for Cs^+. In that case, the number of water molecules in the outer layer, instead of the coordination number, is considered.

The fifth term in the total free energy expression, eq 1, represents the repulsive interactions of the system. These are modeled as hard-core repulsions and can be written in the form

$$\frac{U_{rep}}{V} = \beta\pi(\phi_p + \phi_w + \phi_+ + \phi_- + \phi_{+-}) \tag{9}$$

where π is a repulsive interaction field. The field is determined by the requirement that the total volume is filled with either polymers, solvents, ions, or ion pairs, Namely, we impose the

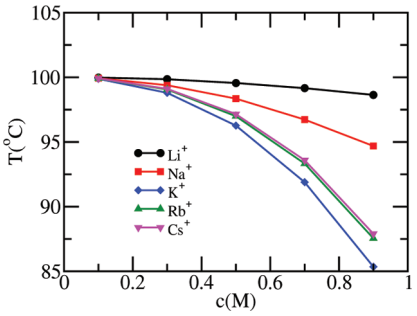

Figure 6. Cloud points of PEO solutions (PEO:water = 1 wt %) as functions of different salt concentrations less than 1 M.

packing constraint associated with the excluded volume interactions having the form

$$\phi_p + \phi_w + \phi_+ + \phi_- + \phi_{+-} = 1 \quad (10)$$

The last term of eq 1 accounts for the electrostatic contribution to the free energy. Although the monovalent ion has a net charge, the closest distance between cation and anion (i.e., the sum of their radius) is usually larger than (in large cations) or close to (in small cations) the Bjerrum length, seen in Table 2. Hence, the electrostatic interactions are neglected here. In reality, the electrostatic contributions are partly included in the hydrogen bonds and the explicit consideration of hydrated ions and ion pairs. However, it is also clear that not all the electrostatic contributions are included.

The total Helmholtz free energy density now becomes

$$\begin{aligned}\frac{\beta F}{V} = {} & \frac{\rho_p}{N}\sum_\alpha P(\alpha)\ln P(\alpha) + \frac{\rho_p}{N}\left[\ln\frac{\rho_p \nu_w}{N} - 1\right] \\ & + \rho_w[\ln \rho_w\nu_w - 1] + \rho_+[\ln \rho_+\nu_w - 1] \\ & + \rho_-[\ln \rho_-\nu_w - 1] + \rho_{+-}[\ln \rho_{+-}\nu_w - 1] \\ & + \frac{\chi}{\nu_w}\phi_p(1-\phi_p) + \sum_j a_j\rho_j\left[\sum_i x_{ij}\ln x_{ij}\right. \\ & \left. + \left(1 - \sum_i x_{ij}\right)\ln\left(1 - \sum_i x_{ij}\right) - \sum_i x_{ij}\beta\Delta F_{ij}\right] \\ & + \sum_i d_i\rho_i\left(1 - \frac{\sum_j x_{ij}a_j\rho_j}{d_i\rho_i}\right)\ln\left(1 - \frac{\sum_j x_{ij}a_j\rho_j}{d_i\rho_i}\right) \\ & - \sum_j a_j\rho_j\sum_i x_{ij}\ln\left(\frac{d_i\rho_i\nu_w}{e}\right) + \beta\pi(\phi_p \\ & + \phi_w + \phi_+ + \phi_- + \phi_{+-} - 1) \end{aligned} \quad (11)$$

where $-\beta\Delta F_{ij}$ is the gain in free energy of forming a single hydrogen bond, which includes the energetic gain and entropic loss: $\beta\Delta F_{ij} = \beta\Delta E_{ij} - \Delta S_{ij}$. According to ref 14, the enthalpy of water−PEO hydrogen bonding free energy $\Delta E_{wp}/k$ is fixed at 2000 K, and the one of water−water $\Delta E_{ww}/k$ is chosen at 1800 K. The entropic loss is related to v_{hb}^{ij} and given by $\Delta S_{ij} = -\ln((1 - \cos\Delta_{ij})/2)$, with $\Delta_{wp} = \pi/8.35$ and $\Delta_{ww} = \pi/4.75$. These parameters were used to get phase diagrams of the bulk PEO solutions, which were in a good agreement with experiments.[14]

In the presence of salt, we choose $\Delta F_{ww} = \Delta F_{w+} = \Delta F_{w-} = \Delta F_{+w} = \Delta F_{++} = \Delta F_{+-}$ and $\Delta F_{wp} = \Delta F_{+p}$. The reason for the former is that these types of hydrogen bonds are formed between water molecules, either free water or bound water, while the latter is hydrogen binding between water (free or bound) and PEO. In eq 11, the average fraction of different hydrogen bonds x_{ij} is introduced, which reflects not only the extent of hydrogen bonding but also the liquid structure of solutions. It is defined as

$$x_{ij} \equiv \frac{n_{ij}}{N_i d_i} \quad (12)$$

where n_{ij} is the number of hydrogen bonds. $N_i d_i$ is a total number of donors provided by species i.

By minimizing the free energy, eq 11, we can get specific expressions of the probability distribution function $P(\alpha)$ of the polymer conformations, densities for different species, and average fractions of hydrogen bonding for equilibrium states, seen in the Appendix. Using these equations, we get the minimal free energy:

$$\begin{aligned}\frac{\beta F_{min}}{V} = {} & -\frac{\rho_p}{N}\ln q + \frac{\rho_p}{N}\left[\ln\frac{\rho_p}{N}\nu_w - 1\right] - \rho_w - \rho_+ \\ & - \rho_- - \rho_{+-} + \frac{\chi}{\nu_w}\phi_p{}^2 - \beta\pi + \sum_i\sum_j x_{ij}a_j\rho_j \end{aligned} \quad (13)$$

From eq 13 two important physical quantities, the chemical potential μ and the osmotic pressure Π, can be obtained by the appropriate deviation from the free energy. They are given by two equations of $\beta\mu = [\partial(\beta F_{min}/V)/\partial\phi_p]_{\phi_+,\phi_-,\phi_{+-}}$ and $\beta\Pi = \beta\mu\phi_p - \beta F_{min}/V$.

The cloud point is the point of phase transition. Below it, the solution is homogeneous with the volume fraction of PEO ϕ_p. Above it, phase separation occurs; that is, the solution separates into a polymer-rich phase with volume fraction (ϕ_{p1}) and a polymer-poor phase with volume fraction (ϕ_{p2}). The cloud point is determined by the equality of chemical potentials of the polymers and osmotic pressures, i.e., $\mu(\phi_{p1}) = \mu(\phi_{p2})$ and $\Pi(\phi_{p1}) = \Pi(\phi_{p2})$. We choose to preform calculations for PEO with the molecular weight of 1 020 000 Da, which shows a cloud point at 100 °C in the pure PEO solution with the concentration of PEO: water = 1 wt %. Using those conditions, we determine the strength of the interaction parameter for which we get $\chi = 117.35/T$. The other parameters that we use in the theory are the volume of water to be 0.03 nm^3 and the one of PEO segment is 0.065 nm^3.

Figure 5a shows the change of cloud points of PEO electrolyte solutions with the addition of different chloride salts at the salt concentration of 0.5 M. The cloud points are not found to be a monotonic function of the size of the ions. According to the extent of the decrease in the cloud point temperature, alkali metal ions can be ranked in the series of $K^+ > Rb^+ > Cs^+ > Na^+ > Li^+$, which agrees with the experimental observations.[20,21] Moreover, the decrease of water−PEO hydrogen bonds, obtained from MD simulations in Figure 4a, is in line with the series, which implies that the decrease of cloud point roots in the breaking of water−PEO hydrogen bonds. The question that arises then is, why does the introduction of salt lead to the decrease of water−PEO hbs? To address this point, the average fractions of cation−PEO (x_{+p}) and cation−water (x_{+w}) are shown in Figure 5b. Both of them show similar behavior, increasing from Li^+ to K^+ and decreasing after K^+. This is because of the largest number of hb donors provided by K^+, seen in Table 2. Meanwhile, we find that x_{+w} is larger than x_{+p} because of $\Delta F_{+w} > \Delta F_{+p}$, which means the

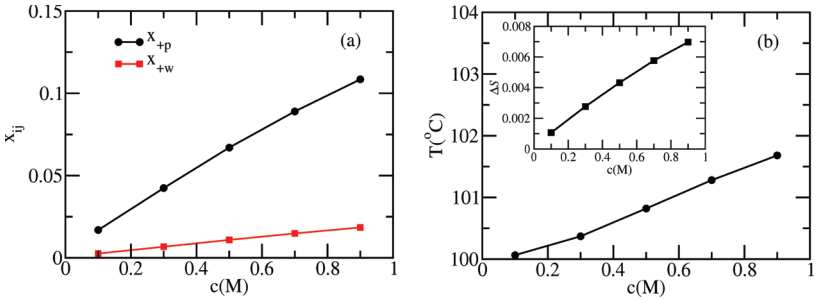

Figure 7. (a) Averaged fractions of cation−PEO (x_{+p}) and cation−water (x_{+w}) hydrogen bonds and (b) cloud points of PEO solutions with the inset of the change of entropy of PEO chains as functions of salt concentrations. All parameters are the same to the case of Li^+, except that the free energy of cation−PEO hydrogen bonding F_{+p} is enlarged.

formation of cation−PEO hydrogen bonds is accompanied by more cation−water hbs. That is, once cations bind to PEO, local water molecules tend to form hydrogen bonds with cations rather than PEO segments. Therefore, the hydrophobicity of PEO is increased.

Figure 6 shows cloud points as functions of salt concentrations. It can be seen that cloud point temperatures show a large decrease at high salt concentrations, in agreement with experiments,[20,21] where both cation−PEO/cation−water hydrogen bonds and steric repulsions of the ions increase. Thus, the salting-out phenomenon is distinct. Note that the specific salt effects on PEO electrolyte solutions still follows the series of K^+ > Rb^+ > Cs^+ > Na^+ > Li^+ for all salt concentrations.

So far we only consider conditions when the alkali mental ions, and cation−water hydrogen bonds are more energetically favorable than cation−PEO hbs. But for other ions and polymers, $\Delta F_{+p} > \Delta F_{+w}$ is also possible. For instance, in PNIPAM electrolyte systems,[50] strong ion PNIPAM binding is observed. Here we choose $\Delta F_{+p} = 2\Delta F_{wp}$ and keep all other parameters the same to the case of Li^+. Our aim is to clarify the possible difference in the macroscopic behavior that arises from the change of microscopic interactions. Figure 7a displays the change of x_{+p} and x_{+w} with the increasing salt concentration. The larger value of x_{+p} is expected due to $\Delta F_{+p} > \Delta F_{+w}$. But the cloud point shows an unexpected behavior, as shown in Figure 7b. Namely, the cloud temperature increases with the increase of salt concentration. This effect indicates the appearance of salting-in. Under this circumstance, the binding of cations to polymers does not result in the formation of a large number of cation−water hydrogen bonds. Therefore, water−polymer hydrogen bonds are not weakened. The inset in Figure 7b shows the increase of entropic difference of the polymer (ΔS) with the increasing of salt concentrations. Thus, salting-in may happen in the case having strong associations between ions and polymers, and the theory can be used to predict either salting-out or salting-in systems, which result from the specific incorporation of the competing interactions.

IV. CONCLUSIONS AND DISCUSSION

The combination of simulation and statistical thermodynamic theory is used to study the specific salt effects in PEO electrolyte solutions. A good example of using this method was done by Luo et al.,[78] who got a perfect agreement of ion distributions near a charged planar surface between theoretical results and X-ray measurements. Furthermore, recent works[79−82] have shown that the method is useful in electrolyte solutions. In the present work, PEO electrolyte solutions have been studied systematically. First, radial distribution functions of ion−water, water−water, EO−water, and EO−ions are extracted from atomic MD simulations, which disclose characters of microscopic structures and interactions of different species. Second, we generalize the molecular theory to PEO electrolyte solutions, which includes the competition between the different interactions and possible hydrogen bonding between the species. Four main characters at the molecular level are taken into account, which are hydrated ion structures, short-ranged hydrogen binding interactions, different abilities for various ions to form hydrogen bonds, and the existence of contact ion pairs. Third, we calculate cloud points of PEO electrolyte solutions and get the salting-out ability for alkali mental ions following the series of K^+ > Rb^+ > Cs^+ > Na^+ > Li^+, as experiments reported. Moreover, our simulation results on the influence of cations on the formation of PEO−water hydrogen bonds also agree with the series. In conclusion, the specific salt effects in PEO electrolyte solutions originate in the competition among cation−PEO, cation−water, and water−PEO hydrogen bonds as well as the impact of steric repulsions of ions. The macroscopic behaviors of electrolyte solutions, such as salting-out and salting-in, are verified in the results of microscopic structures and interactions.

Regarding the accuracy of the model, we should mention that only monovalent ions and moderate concentrations (<1 M) are considered here. For much higher salt concentrations, ion clusters cannot be avoided, which are not included in the present model. For multivalent ions their hydration structures become complicated. These challenges are still open. However, this is a successful try to explore the mechanism of specific salt effects in PEO solutions with moderate salt concentrations by the combined method, in which specific simulation information is incorporated within a thermodynamic consistent framework with which systematic studies can be carried out.

APPENDIX

The number of donors/acceptors per bound water results from the competition between ion−water and water−water interactions within the first hydration shell. For small cations, such as Li^+ and Na^+, the molecular dipole of each bound water molecule tends to align along the cation−oxygen line under the influence of strong ion−water interactions, and two hydrogens remain as two donors for the hydrogen binding with other molecules. For K^+, ion−water interactions become comparable to water−water interactions. The reorientation of bound water is not distinct, where each bound water molecule is assumed to offer two donors as well as one acceptor. For a large cation, like Rb^+, water−water interactions exceed ion−water interactions

even in the first hydration shell. Except for hydrogen bonds between bound water themselves within the first hydration shell, each bound water is assumed to provide one donor and one acceptor for the hydrogen bonding with other molecules. For the largest cation Cs^+, the ion−water interactions become very weak so that the averaged distance between Cs^+ and water is larger than that of two water molecules. The formation of two-layer structure of bound water molecules within the first hydration shell, called open-work structure,[83−86] is observed. Typically, four water molecules stay in the inner layer, and others remain in the outer layer. Hence, only bound water molecules in the outer layer have contributions to the hydrogen bonding between Cs^+ and other molecules. Each of them offers one donor and one acceptor too. For Cl^-, its bound water is suggested to provide two acceptors because the reorientation of the bound water under the influence of the negative charge leads to the oxygen out of the hydration shell for hydrogen binding with other molecules. This also is the reason why no associations between anions and PEO are observed in Figure 4c. Contact ion pairs do not provide donors/acceptors since bound water are strongly reoriented under the influence both from cation and anion.

Different expressions by the minimization of free energy, eq 11, are shown in the following. The probability distribution function $P(\alpha)$ of the polymer conformations yields

$$P(\alpha) = \frac{1}{q}\exp\left[-\frac{\chi}{v_w}Nv_p(1.0-2\phi_p) - \beta\pi Nv_p - 2N\ln(1-\sum_i x_{ip})\right] \quad (14)$$

where q is a normalization constant ensuring $\sum_\alpha P(\alpha) = 1$. It can be concluded from the equation of $P(\alpha)$ is independent of the conformation, and therefore, unlike the theory in inhomogeneous environments, the conformations of the chains do not change their probability depending on the solution. Thus, the chain conformations are uncoupled to the thermodynamics.

Densities of free water, cation, anion, and contact ion pair are given as in the following:

$$\rho_w = \frac{1}{v_w}\exp\left[-\beta\pi v_w - 2\ln(1-\sum_i x_{iw}) - 2\ln\left(1-\frac{\sum_j x_{wj}a_j\rho_j}{2\rho_w}\right)\right] \quad (15)$$

$$\rho_+ = \frac{1}{v_w}\exp\left[-\beta\pi v_+ - a_+\ln(1-\sum_i x_{i+}) - d_+\ln\left(1-\frac{\sum_j x_{+j}a_j\rho_j}{d_+\rho_+}\right)\right] \quad (16)$$

$$\rho_- = \frac{1}{v_w}\exp\left[-\beta\pi v_- - a_-\ln(1 - \sum_i x_{i-}) - d_-\ln\left(1-\frac{\sum_j x_{-j}a_j\rho_j}{d_-\rho_-}\right)\right] \quad (17)$$

and

$$\rho_{+-} = \frac{1}{v_w}\exp[-\beta\pi v_{+-}] \quad (18)$$

The average fractions of hydrogen bonding among different species are

$$0 = \ln x_{ij} - \ln(1-\sum_i x_{ij}) - \beta\Delta F_{ij} - \ln\left[1-\frac{\sum_j x_{ij}a_j\rho_j}{d_i\rho_i}\right] - \ln d_i\rho_i v_w \quad (19)$$

From eqs 15 to 17, it is concluded that densities of free water, cation, and anion rely on the fractions of hydrogen bonding, while eq 18 reflects the density of contact ion pair originating in the osmotic pressure of the solution and does not relate to the hydrogen bonding, because contact ion pairs provide neither donors nor acceptors. Moreover, eq 19 indicates that average fractions of hydrogen bonding relating to the density of species, which can offer donors or acceptors. So densities of different species for PEO−salt solutions and average fractions of hydrogen bonding are coupled in a nonlinear way.

AUTHOR INFORMATION

Corresponding Author
*E-mail: myqiang@nju.edu.cn.

ACKNOWLEDGMENT

This work is supported by the National Natural Science Foundation of China under Grants 10804045, 91027040, and 10974080. I.S. acknowledges support from the National Institute of Health of the US under Grant EB005772. We are grateful to the high performance computing center of Nanjing University for doing the numerical calculations in this paper on its IBM blade cluster system. C.-L. Ren thanks Dr. Z.-Y. Wang for the insightful discussions.

REFERENCES

(1) Malcolm, G. N.; Rowlinson, J. S. *Trans. Faraday. Soc.* **1957**, *53*, 921.
(2) Bailey, F. E.; Callard, R. W. *J. Appl. Polym. Sci.* **1959**, *1*, 56.
(3) Saeki, S.; Kuwahara, N.; Nakata, M.; Kaneko, M. *Polymer* **1976**, *17*, 685.
(4) Bae, Y. C.; Lambert, S. M.; Soane, D. S.; Prausnitz, J. M. *Macromolecules* **1991**, *24*, 4403.
(5) Albertsson, P. A. *Partition of Cell Particles and Macromolecules*, 3rd ed.; Wiley: New York, 1986.
(6) Rogers, R. D., Eiteman, M. A., Eds. *Aqueous Biphasic Separations: Biomolecules to Metal Ions*; Plenum Press: New York, 1995.
(7) Bieze, T. W. N.; Barnes, A. C.; Huige, C. J. M.; Enderby, J. E.; Leyte, J. C. *J. Phys. Chem.* **1994**, *98*, 6568.
(8) Venohr, H.; Fraaije, V.; Strunk, H.; Borchard, W. *Eur. Polym. J.* **1998**, *34*, 723.
(9) Magazú, J. *J. Mol. Struct.* **2000**, *523*, 47.
(10) Karlström, G. *J. Phys. Chem.* **1985**, *89*, 4962.
(11) Matsuyama, A.; Tanaka, F. *Phys. Rev. Lett.* **1990**, *65*, 341.
(12) Bekiranov, S.; Bruinsma, R.; Pincus, P. *Phys. Rev. E* **1997**, *55*, 577.
(13) Baulin, V. A.; Halperin, A. *Macromolecules* **2002**, *35*, 6432.

(14) Dormidontova, E. E. *Macromolecules* **2002**, *35*, 987.
(15) Jeppesen, C.; Kremer, K. *Europhys. Lett.* **1996**, *34*, 563.
(16) Smith, G. D.; Bedrov, D.; Borodin, O. *J. Am. Chem. Soc.* **2000**, *122*, 9548.
(17) Smith, G. D.; Bedrov, D. *J. Phys. Chem. B* **2003**, *107*, 3095.
(18) Smith, G. D.; Bedrov, D.; Borodin, O. *Phys. Rev. Lett.* **2000**, *85*, 5583.
(19) Cohen Stuart, M. A.; Huck, W. T. S.; Genzer, J.; Müller, M.; Ober, C.; Stamm, M.; Sukhorukov, G. B.; Szleifer, I.; Tsukruk, V. V.; Urban, M.; Winnik, F.; Zauscher, S.; Luzinov, I.; Minko, S. *Nature Mater.* **2010**, *9*, 101.
(20) Florin, B. E.; Kjellander, R.; Eriksson, J. C. *J. Chem. Soc., Faraday Trans. 1* **1984**, *80*, 2889.
(21) Ananthapadmanabhan, K. P.; Goddard, E. D. *Langmuir* **1987**, *3*, 25.
(22) Tello, P. G.; Gomacho, F.; Blazquez, G. *J. Chem. Eng. Data* **1994**, *39*, 611.
(23) Mei, L. H.; Lin, D. Q.; Zhu, Z. Q.; Han, Z. X. *J. Chem. Eng. Data* **1995**, *40*, 1168.
(24) Nozary, S.; Modarress, H.; Eliassi, A. *J. Appl. Polym. Sci.* **2003**, *89*, 1983.
(25) Hey, M. J.; Jackson, D. P.; Yan, H. *Polymer* **2005**, *46*, 2567.
(26) Hofmeister, F. *Arch. Exp. Pathol. Pharmakol.* **1888**, *24*, 247.
(27) Bockris, J.; Reddy, A. K. N. *Modern Electrochemistry*; Plenum: New York, 1970.
(28) Franks, F., Ed. *Water: A Comprehensive Treatise*; Plenum: London, 1973; Vol. 3.
(29) Schuster, P.; Zundel, G.; Sandorfy, C. *The Hydrogen Bond*; Elsevier: Amsterdam, 1976.
(30) Marcus, Y. *Ion Solvation*; Wiley: Chichester, UK, 1985.
(31) Krestov, G. A. *Thermodynamics of Solvation*; Ellis Horwood: Chichester, UK, 1991.
(32) Bostrom, M.; Williams, D. R. M.; Ninham, B. W. *Biophys. J.* **2003**, *85*, 686.
(33) Wondrak, E. M.; Louis, J. M.; Oroszlan, S. *FEBS Lett.* **1991**, *280*, 344.
(34) Lo Nostro, P.; Ninham, B. W.; Lo Nostro, A.; Pesavento, G.; Fratoni, L.; Baglioni, P. *Phys. Biol.* **2005**, *2*, 1.
(35) Zhang, Y.; Cremer, P. S. *Curr. Opin. Chem. Biol.* **2006**, *10*, 658.
(36) Kunz, W. *Pure Appl. Chem.* **2006**, *78*, 1611.
(37) Kunz, W.; Lo Nostro, P.; Ninham, B. W. *Curr. Opin. Colloid Interface Sci.* **2004**, *9*, 1.
(38) Collins, K. D.; Neilson, G. W.; Enderby, J. E. *Biophys. Chem.* **2007**, *128*, 95.
(39) Ball, P. *Chem. Rev.* **2008**, *108*, 74.
(40) Omta, A. W.; Kropman, M. F.; Woutersen, S.; Bakker, H. J. *Science* **2003**, *301*, 347.
(41) Kropman, M. F.; Bakker, H. J. *J. Am. Chem. Soc.* **2004**, *126*, 9135.
(42) Smith, J. D.; Saykally, R. J.; Geissler, P. *J. Am. Chem. Soc.* **2007**, *129*, 13847.
(43) Vlachy, N.; Jagoda-Cwiklik, B.; Vácha, R.; Touraud, D.; Jungwirth, P.; Kunz, W. *Adv. Colloid Interface Sci.* **2009**, *146*, 42.
(44) Degrève, L.; da Silva, F. L. B. *J. Chem. Phys.* **1999**, *110*, 3070.
(45) Guardia, E.; Laria, D.; Marti, J. *J. Phys. Chem. B* **2006**, *110*, 6332.
(46) Krekeler, C.; Delle Site, L. *J. Phys.: Condens. Matter* **2007**, *19*, 192101.
(47) Nag, A.; Chakraborty, D.; Chandra, A. *J. Chem. Sci.* **2008**, *120*, 71.
(48) Zangi, R.; Berne, B. J. *J. Phys. Chem. B* **2006**, *110*, 22736.
(49) Zangi, R.; Hagen, M.; Berne, B. J. *J. Am. Chem. Soc.* **2007**, *129*, 4678.
(50) Zhang, Y.; Furyk, S.; Bergbreiter, D. E.; Cremer, P. S. *J. Am. Chem. Soc.* **2005**, *127*, 14505.
(51) Xu, L.; Li, X.; Zhai, M.; Huang, L.; Peng, J.; Li, J.; Wei, G. *J. Phys. Chem. B* **2007**, *111*, 3391.
(52) Kunz, W. *Curr. Opin. Colloid Interface Sci.* **2010**, *15*, 34.
(53) Pitzer, K. S.; Mayorga, G. *J. Phys. Chem.* **1973**, *77*, 2300.
(54) Chen, C. C.; Evans, L. B. *AIChE J.* **1986**, *32*, 444.
(55) Papaiconomous, N.; Simonin, J. P.; Bernard, O.; Kunz, W. *Phys. Chem. Chem. Phys.* **2002**, *4*, 4435.
(56) Boström, M.; Williams, D. R. M.; Ninham, B. W. *Phys. Rev. Lett.* **2001**, *87*, 168103.
(57) Simonin, J. P.; Blum, L.; Turq, P. *J. Phys. Chem.* **1996**, *100*, 7704.
(58) Blum, L.; Vericat, F.; Fawcett, W. R. *J. Chem. Phys.* **1992**, *96*, 3039.
(59) McDonald, N. A.; Jorgensen, W. L. *J. Phys. Chem. B* **1998**, *102*, 8049.
(60) Briggs, J. M.; Matsui, T.; Jorgensen, W. L. *J. Comput. Chem.* **1990**, *11*, 958.
(61) Laasone, K.; Klein, M. L. *J. Chem. Soc., Faraday Trans.* **1995**, *91*, 2633.
(62) Chandrasekhar, J.; Spellmeyer, D. C.; Jorgensen, W. L. *J. Am. Chem. Soc.* **1984**, *106*, 903.
(63) Lindahl, E.; Hess, B.; van der Spoel, D. *J. Mol. Model.* **2001**, *7*, 306.
(64) Degeve, L.; Quintale, C. *J. Chem. Phys.* **1994**, *101*, 2319.
(65) Degeve, L.; da Silva, F. L. B. *J. Mol. Liq.* **2000**, *87*, 217.
(66) Mezei, M.; Beveridge, D. L. *J. Chem. Phys.* **1981**, *74*, 622.
(67) Mezei, M.; Beveridge, D. L. *J. Chem. Phys.* **1981**, *74*, 6902.
(68) Skipper, N. T.; Neilson, G. W. *J. Phys.: Condens. Matter* **1989**, *1*, 4141.
(69) Kiriukhin, M. Y.; Collins, K. D. *Biophys. Chem.* **2002**, *99*, 155.
(70) Mason, P. E.; Neilson, G. W.; Dempsey, C. E.; Barnes, A. C.; Cruickshank, J. M. *Proc. Natl. Acad. Sci. U.S.A.* **2003**, *100*, 4557.
(71) Bouazizi, S.; Nasr, S. *J. Mol. Struct.* **2007**, *837*, 206.
(72) Bouazizi, S.; Nasr, S.; Jaîdane, N.; Bellissent-Funel, M.-C. *J. Phys. Chem. B* **2006**, *110*, 23515.
(73) Lyubartsev, A. P.; Laaksonen, A. *J. Phys. Chem.* **1996**, *100*, 16410.
(74) Mizoguchi, A.; Ohshima, Y.; Endo, Y. *J. Am. Chem. Soc.* **2003**, *125*, 1716.
(75) Hakem, I. F.; Lai, J. *Europhys. Lett.* **2003**, *64*, 204.
(76) Ren, C.-L.; Nap, R. J.; Szleifer, I. *J. Phys. Chem. B* **2008**, *112*, 16238.
(77) Veytsman, B. A. *J. Phys. Chem.* **1990**, *94*, 8499.
(78) Luo, G.; Malkova, S.; Yoon, J.; Schultz, D. G.; Lin, B.; Meron, M.; Benjamin, I.; Vanýsek, P.; Schlossman, M. L. *Science* **2006**, *311*, 216.
(79) Horinek, D.; Netz, R. R. *Phys. Rev. Lett.* **2007**, *99*, 226104.
(80) Lima, E. R. A.; Horinek, D.; Netz, R. R.; Biscaia, E. C.; Tavares, F. W.; Kunz, W.; Boström, M. *J. Phys. Chem. B* **2008**, *112*, 1580.
(81) Lima, E. R. A.; Boström, M.; Horinek, D.; Biscaia, , E. C.; Kunz, W.; Tavares, F. W. *Langmuir* **2008**, *24*, 3944.
(82) Horinek, D.; Serr, A.; Bonthuis, D. J.; Boström, M.; Kunz, W.; Netz, R. R. *Langmuir* **2008**, *24*, 1271.
(83) Tamura, Y.; Yamaguchi, T.; Okada, I.; Ohtaki, H. *Z. Naturforsch., A: Phys. Sci.* **1987**, *42*, 367.
(84) Novikov, A. G.; Rodnikova, M. N.; Savostin, V. V.; Sobolev, O. V. *J. Mol. Liq.* **1999**, *82*, 83.
(85) Ramos, S.; Neilson, G. W.; Barnes, A. C.; Buchanan, P. *J. Chem. Phys.* **2005**, *123*, 214501.
(86) Smirnov, P. R.; Trostin, V. N. *Zh. Obshch. Khim.* **2007**, *77*, 1955.

NOTE ADDED AFTER ASAP PUBLICATION

This paper was published on the Web on February 14, 2011, with minor errors in equation 19. The corrected version was reposted on February 17, 2011.